
¹¹C-Cetrozole: An Improved C-¹¹C-Methylated PET Probe for Aromatase Imaging in the Brain

Kayo Takahashi¹, Takamitsu Hosoya², Kayo Onoe¹, Hisashi Doi¹, Hiroko Nagata¹, Toshiyuki Hiramatsu³, Xiao-Le Li³, Yumiko Watanabe¹, Yasuhiro Wada¹, Tadayuki Takashima¹, Masaaki Suzuki¹, Hirotaka Onoe¹, and Yasuyoshi Watanabe¹

¹RIKEN Center for Life Science Technologies, Hyogo, Japan; ²Institute of Biomaterials and Bioengineering, Tokyo Medical and Dental University, Tokyo, Japan; and ³Department of Biological Information, Graduate School of Bioscience and Biotechnology, Tokyo Institute of Technology, Tokyo, Japan

Aromatase (an enzyme that converts androgens to estrogens) in the brain is involved in neuroprotection, synaptic plasticity, and regulation of sexual and emotional behaviors. To investigate the physiologic and pathologic importance of aromatase in the brain, including in humans, we here report the development of a novel PET probe for aromatase, ¹¹C-cetrozole, which allows noninvasive quantification of aromatase expression. **Methods:** ¹¹C-cetrozole was synthesized by the C-¹¹C-methylation method developed by our group. In vitro autoradiography of frozen sections and a binding study with rat brain homogenates were conducted to demonstrate the specific binding and the dissociation constant. PET studies with anesthetized rhesus monkeys were performed to analyze the dynamics in the brain. **Results:** In vitro and in vivo studies using ¹¹C-cetrozole showed its superiority in brain aromatase imaging in terms of specificity and selectivity, compared with previously developed ¹¹C-vorozole. PET studies showed that ¹¹C-cetrozole had a higher signal-to-noise ratio, providing a sharper image than ¹¹C-vorozole, because the radioactive metabolite of ¹¹C-vorozole was taken up into the brain. High specific binding of ¹¹C-cetrozole was observed in the amygdala and hypothalamus, and we also noted binding in the nucleus accumbens of rhesus monkeys for the first time. **Conclusion:** These results suggest that PET imaging with newly developed ¹¹C-cetrozole is suitable for quantifying the expression of brain aromatase in vivo, possibly providing critical information regarding the functional roles of aromatase in human neurologic and emotional disorders.

Key Words: aromatase; amygdala; hypothalamus

J Nucl Med 2014; 55:852–857

DOI: 10.2967/jnumed.113.131474

Aromatase, an estrogen synthetic enzyme that converts testosterone and androstenedione to estradiol and estrone (1), is considered to play an important role in various brain functions. Studies using aromatase knockout mice demonstrated that aromatase deficiency

leads to susceptibility of neurons to neuronal apoptosis in the frontal cortex of aged females (2) and in the hypothalamus of aged males (3). These mice are also susceptible to neuronal toxins such as domoic acid (4) and 1-methyl-4-phenyl-1,2,3,6-tetrahydropyridine, which is used to produce animal models of Parkinson's disease (5). In behavior studies, aromatase knockout mice exhibit depressive-like behavior (6), aggressive behaviors leading to infanticide (7,8), repressed aggression to intruders (9,10), impaired spatial reference memory (11), and disrupted sexual behavior (7,10). These impaired behaviors can be considerably recovered by specifically introducing human aromatase into the brain of aromatase knockout mice, strongly suggesting a relationship between aromatase and brain functions (9). A relationship between aromatase and Alzheimer's disease or autism was also suggested (12,13). In normal conditions, aromatase is expressed in neurons, but after brain injury, neogenetic aromatase is expressed in astrocytes, which are considered to protect neurons (14). Although these results suggest the importance of local estrogen biosynthesis in the brain, the precise roles of aromatase in neurologic and emotional disorders are not fully understood.

Studying the relationships between aromatase and brain functions would be aided by the ability to obtain quantitative measurements of the expression level and the ability to localize aromatase directly in living animals and humans. For this purpose, the Uppsala University group developed the first PET probe, ¹¹C-vorozole, based on the aromatase inhibitor developed for breast cancer therapy (15). In collaboration with them, we first succeeded in obtaining sufficient PET images in the rhesus monkey brain in which specific binding of ¹¹C-vorozole was detected in the amygdala and hypothalamic regions (16). A method for isolating ¹¹C-vorozole labeled in the right position was established later on (17). Up to now, using ¹¹C-vorozole, the distribution of aromatase in the brain of rats, rhesus monkeys (16), baboons (17), and humans (18) and the effect of anabolic-androgenic steroids on aromatase (19,20) have been demonstrated. Although ¹¹C-labeled sulfonamide analogs (21), ¹¹C-labeled sulfamate derivatives (dual aromatase–steroid sulfatase inhibitors) (22), and ¹¹C-letrozole (23) have also been developed as aromatase imaging PET probes, ¹¹C-vorozole is still the most popular probe for imaging brain aromatase. However, ¹¹C-vorozole has some drawbacks. First, the greatest disadvantage is that a certain amount of nonspecific signal is observed in PET studies. This may be caused by metabolic cleavage of the N-¹¹C-methyl bond followed by unintended reuptake of the radioactive metabolite into the brain. Second, the precursor of ¹¹C-vorozole, norvorozole, is not easily available. Although we have recently established a practical preparative method (24), synthesis of ¹¹C-vorozole still requires a multistep procedure and optical resolution of the racemic mixture.

Received Aug. 22, 2013; revision accepted Jan. 21, 2014.
For correspondence or reprints contact either of the following:
Yasuyoshi Watanabe, RIKEN Center for Life Science Technologies, 6-7-3 Minatojima-Minamimachi, Chuo-ku, Kobe, Hyogo 650-0047, Japan.
E-mail: yuwata@riken.jp
Takamitsu Hosoya, Institute of Biomaterials and Bioengineering, Tokyo Medical and Dental University, 2-3-10 Kanda-Surugadai, Chiyoda-ku, Tokyo 101-0062, Japan.
E-mail: thosoya.cb@tmd.ac.jp
Published online Mar. 27, 2014.
COPYRIGHT © 2014 by the Society of Nuclear Medicine and Molecular Imaging, Inc.

And third, it was reported that all 3 possible N-¹¹C-methylation at the triazole moiety of norvorozole proceeded in the reaction with ¹¹C-CH₃I, decreasing the yield and complicating isolation of the desired probe (17).

To address these issues and explore a novel PET probe for aromatase imaging, we focused on YM511, an aminotriazole derivative developed as an aromatase inhibitor for breast cancer (25). Because this compound showed high inhibitory competence with a half maximal inhibitory concentration (IC₅₀) of 0.12 nM for human placental aromatase and had a simple structure that was easy to synthesize, we planned to modify and optimize this compound to obtain a more efficient PET probe. Here, we describe the development of a new probe, named ¹¹C-cetrozole, in which the bromophenyl moiety of YM511 was changed to an ¹¹C-methylphenyl group. The new compound works better than ¹¹C-vorozole, with improved characteristics suitable for brain aromatase imaging.

MATERIALS AND METHODS

Synthesis of Pinacol Boranyl Precursor 1 and Tributylstannyl Precursor 3 for ¹¹C-Cetrozole (¹¹C-2) and Nonradiolabeled Cetrozole (2)

Detailed procedures are provided in the supplemental data (available at <http://jnm.snmjournals.org>).

Synthesis of ¹¹C-Cetrozole (¹¹C-2) (Fig. 1)

¹¹C-carbon dioxide was produced by a ¹⁴N(p,α)¹¹C reaction using a cyclotron (CYPRIS HM-18; Sumitomo Heavy Industries Ltd.) and then converted to ¹¹C-methyl iodide by treatment with lithium aluminum hydride, followed by hydriodic acid. The obtained ¹¹C-methyl iodide was used for palladium(0)-mediated rapid ¹¹C-methylation as follows (26).

¹¹C-methyl iodide was transferred by a stream of helium gas (30 mL/min) into a solution of boron precursor **1** (4.0 mg, 10 μmol), Pd₂(dba)₃ (2.9 mg, 2.5 μmol), P(*o*-tolyl)₃ (4.0 mg, 13 μmol), and K₂CO₃ (4.0 mg, 30 μmol) in dimethylformamide (0.5 mL) at room temperature. The resulting mixture was heated at 65°C for 2 min. Salts and palladium residue in the reaction mixture were removed by a solid-phase extraction, washing with 1 mL of a solution of CH₃CN:30 mM CH₃COONH₄ (35:65). The combined elutes were injected into preparative high-performance liquid chromatography (HPLC) with a γ detector (mobile phase: CH₃CN:30 mM CH₃COONH₄ [35:65]; column: COSMOSIL AR-II C18 [Nacalai], 10 × 250 mm; guard column: SUMIPAX Filter PG-ODS [Sumika]; flow rate: 6 mL/min; ultraviolet detection: 254 nm; retention time of ¹¹C-2: 13.5 min). The desired fraction was collected into a flask, and then the organic solvent was removed under reduced pressure. The desired ¹¹C-labeled compound was dissolved in a mixture of polysorbate 80 (0.05 mL), propylene glycol (0.3 mL), and saline (4 mL). The total synthesis time including HPLC purification and radiopharmaceutical formulation for intravenous administration was 30 min. The radioactivity of ¹¹C-2 prepared for administration was 2.6–6.2 GBq, and the specific radioactivity was 90–127 GBq/μmol. The identification of ¹¹C-2 was confirmed by coinjection with the unlabeled authentic sample on analytic HPLC with a γ detector (mobile phase: CH₃CN:30 mM CH₃COONH₄ [40:60]; column: COSMOSIL AR-II C18 [Nacalai], 4.6 × 100 mm; flow rate: 1 mL/min; ultraviolet detection: 254 nm; retention time of ¹¹C-2: 4.5 min). The chemical purity and the radiochemical purity were greater than 95%. The decay-corrected yield based on ¹¹CH₃I in a reaction vial was 54%–60%.

¹¹C-cetrozole could also be prepared efficiently from tributylstannyl precursor **3** (Supplemental Fig. 1).

Synthesis of ¹¹C-Vorozole

¹¹C-vorozole was synthesized according to a previously published procedure (17) using norvorozole as the precursor (24). The specific

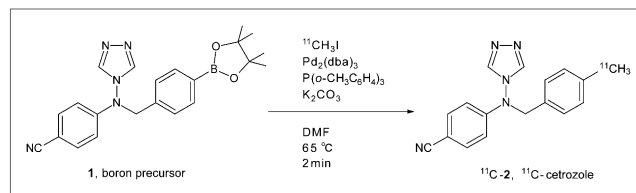


FIGURE 1. Radiosynthesis of ¹¹C-cetrozole (¹¹C-2) by rapid ¹¹C-methylation using pinacol boranyl precursor **1**. DMF = dimethylformamide.

radioactivities were in the range of 22–90 GBq/μmol, and the radiochemical purity was greater than 99.5%.

Animals

Male and female Sprague–Dawley rats (8–12 w) were housed under constant temperature and humidity and were maintained under a 12-h light–dark cycle with free access to water and food. Male adult rhesus monkeys (*Macaca mulatta*; weight, 4.6–7.1 kg) were housed individually, food was given twice a day, and water was available ad libitum. Animals were maintained and handled in accordance with the recommendations of the U.S. National Institutes of Health, and the study was approved by the Animal Care and Use Committee of Kobe Institute at RIKEN (MAH18-05, MAH21-13, MAH21-10).

In Vitro Assays Using ¹¹C-Cetrozole

In vitro autoradiography using rat brain sections was performed as described previously (16). The method is described in the legend to Supplemental Figure 2.

Ligand saturation experiments with brain homogenate were performed as described previously (16) with suitable modifications. The method is described in the legend to Supplemental Figure 3.

PET Studies

PET scans were obtained with monkeys using ¹¹C-cetrozole ($n = 4$) or ¹¹C-vorozole ($n = 5$). All monkeys were used for the tracer dose studies, and 2 monkeys were used for one additional blocking study with unlabeled vorozole at a dose of 150 μg/kg. The monkeys were sedated with ketamine hydrochloride (15 mg/kg, intramuscularly), and venous cannulae were placed in the saphenous veins for further continuous anesthesia with propofol (10 mg/kg/h) and PET tracer injection. Before the emission scan, a transmission scan was obtained for 30 min for attenuation correction. Each tracer (¹¹C-cetrozole, 106–535 MBq; ¹¹C-vorozole, 117–231 MBq) was administered intravenously as a bolus. The monkeys were scanned for 90 min (4 × 30, 3 × 60, 2 × 150, 2 × 300, and 7 × 600 s) using a microPET Focus 220 (Siemens). For quantitative data analysis with an input function, 2 monkeys underwent additional PET with arterial blood sampling at the following time points: 8, 16, 24, 32, 40, 48, 56, 64, 72, 90, and 150 s and 4, 6, 10, 20, 30, 45, 60, and 90 min. The samples at 64 s and 10, 20, 30, and 60 min were also used for metabolite analysis.

Analysis of Radiolabeled Metabolites in Brain and Plasma

Rats received radioactivity (~110 MBq/body) and were sacrificed at 5-, 10-, and 20-min time points ($n = 3$ at each time point). Plasma and whole brains, which were removed immediately and homogenized in water, were used for analyses of ¹¹C-cetrozole and ¹¹C-vorozole metabolites. The plasma of 2 monkeys was taken at time points of 64 s and 4, 10, 20, 30, and 60 min during PET scans and used for analyses of ¹¹C-cetrozole and ¹¹C-vorozole metabolites. Measurements of radiolabeled metabolites in the brain and plasma were performed as described previously (27).

Analysis of PET Data

For quantitative analysis of PET images (i.e., kinetic modeling), PMOD software (PMOD Technologies Ltd.) was used. Volumes of

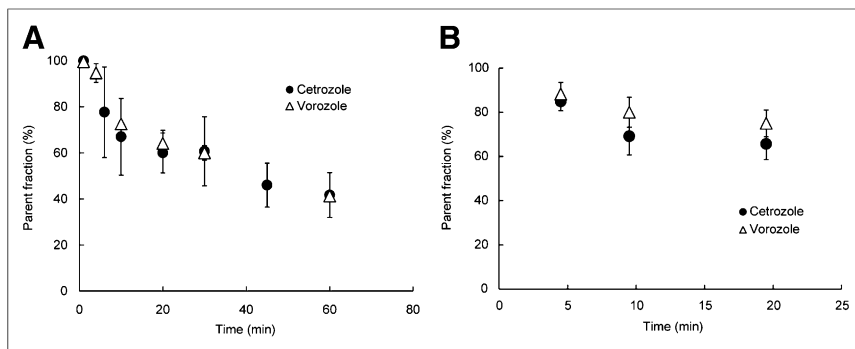


FIGURE 2. Elimination curve of intact ¹¹C-cetozole in plasma of rhesus monkeys (A, *n* = 4, mean ± SEM) and rat (B, *n* = 3, mean ± SEM). ¹¹C-cetozole was metabolized over time as much as ¹¹C-vorozole. Curve was fitted to percentage of intact ¹¹C-cetozole.

interest were delineated in the cerebellum, amygdala, hypothalamus, nucleus accumbens, thalamus, white matter, and temporal cortex. Decay-corrected time–activity curves were generated for each brain region and arterial blood plasma and parent compound. The time–activity curves for plasma and metabolites were fitted to a 3 exponential model and a Hill function, respectively. The data with arterial blood sampling were analyzed with a Logan plot (28), and the total distribution volume (V_t) in each brain region was calculated. The data without arterial blood sampling were analyzed with a Logan reference tissue model based on average *k*₂' (29), using the cerebellum as a reference. Nondisplaceable binding potential (BP_{nd}) and distribution volume ratio (DVR), which are linear functions of enzyme availability, were calculated.

RESULTS

In Vitro Assays Using ¹¹C-Cetozole and Biodistribution

In an autoradiographic study with ¹¹C-cetozole of the rat brain, a high level of binding was observed in the medial amygdala and bed nucleus of the stria terminalis, and a moderate level of binding was seen in the hypothalamus similar to the study with ¹¹C-vorozole (Supplemental Fig. 2) (16). The binding was clearly displaced by application of excess amounts of unlabeled vorozole. Little signal was detected in other brain regions including the cerebellum. Male rats showed higher binding of ¹¹C-cetozole in the medial amygdala and bed nucleus of stria terminalis than female rats (Supplemental Fig. 3).

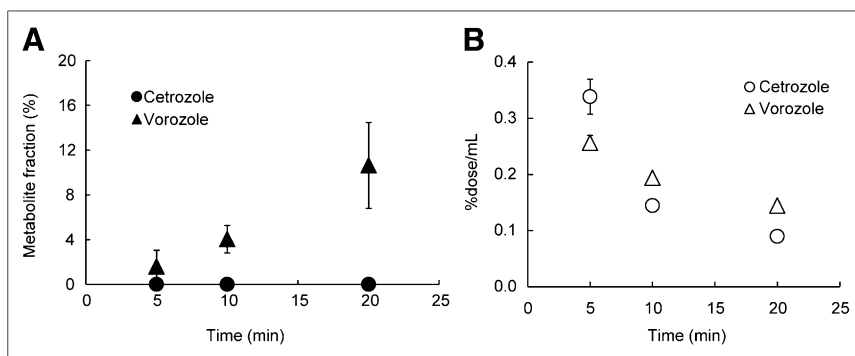


FIGURE 3. Radiolabeled metabolite fraction (A, *n* = 3, mean ± SEM) and time–activity of ¹¹C-cetozole and ¹¹C-vorozole (B, *n* = 3, mean ± SEM) in rat brain. (A) Radiolabeled metabolite of ¹¹C-cetozole was not detected even 20 min after injection of radioactivity, in contrast to ¹¹C-vorozole for which radiolabeled metabolite accumulated in brain over time. (B) Both ¹¹C-cetozole and ¹¹C-vorozole were eliminated from brain over time.

The Scatchard plot analysis of ¹¹C-cetozole in the rat medial amygdala showed a single binding site of aromatase with the binding affinity (*K*_d) value of 0.11 ± 0.02 nM (*n* = 3) (Supplemental Fig. 4).

The biodistribution of ¹¹C-cetozole in rats showed relatively high accumulation in the small intestine at 30 min after the administration (Supplemental Fig. 5).

Analysis of ¹¹C-Cetozole and ¹¹C-Vorozole Metabolites in Brain and Plasma

The proportions of the parent compound in plasma decreased over time, and we observed no difference between ¹¹C-cetozole and ¹¹C-vorozole in both monkeys and rats (Fig. 2). At 30 min after administration of the tracers, about 60% of ¹¹C-cetozole and ¹¹C-vorozole remained intact; the level was about 40% at 60 min in rhesus monkey plasma (Fig. 2A). Similarly, we found no difference between the proportions of the parent compound of each tracer in the plasma of rats (Fig. 2B). To also investigate metabolites in the brain, the radiolabeled parent compound and metabolites were measured in the rat brain. Although radiolabeled metabolites of ¹¹C-vorozole accumulated in the brain over time, radiolabeled metabolites of ¹¹C-cetozole were not detected even 20 min after administration of the tracer (Fig. 3). Representative radiochromatograms are shown in Supplemental Figure 6. ¹¹C-cetozole and ¹¹C-vorozole with retention times of 3.0 and 2.6 min gave one major metabolite at 3.7 and 0.4–0.5 min, respectively. The amount of ¹¹C-vorozole metabolite increased over time both in plasma and in brain. In contrast, ¹¹C-cetozole metabolites accumulated only in plasma but not in the brain.

PET Studies

DVR images of ¹¹C-cetozole and ¹¹C-vorozole showed higher binding activity in the amygdala with both PET tracers (Fig. 4). However, the accumulation of the radiotracers in the amygdala and hypothalamus was delineated more clearly with ¹¹C-cetozole than with ¹¹C-vorozole. Additionally, the nucleus accumbens was clearly delineated only with ¹¹C-cetozole. Time–activity curves showed that the clearance rate of ¹¹C-vorozole was slower than that of ¹¹C-cetozole, especially in the late phase (Fig. 5). The standardized uptake value (SUV) of ¹¹C-vorozole plateaued after 30 min of scan time, and that in the amygdala and nucleus accumbens seemed to slightly increase until 90 min (Fig. 5B). The SUV of ¹¹C-cetozole continued to decrease (Fig. 5A).

The BP_{nd} of ¹¹C-cetozole was high in the amygdala, hypothalamus, and nucleus accumbens (Fig. 6A). In these 3 regions, the BP_{nd} of ¹¹C-vorozole was also high, although relatively low BP_{nd} was observed in the hypothalamus (Fig. 6B). The BP_{nd} in the cortices was low with both tracers. Most of the signals in the white matter could be regarded as nonspecific binding. The BP_{nd} of ¹¹C-cetozole was higher than that of ¹¹C-vorozole by 88%, 170%, and 55% in the amygdala, hypothalamus, and nucleus accumbens, respectively. ¹¹C-cetozole also showed better

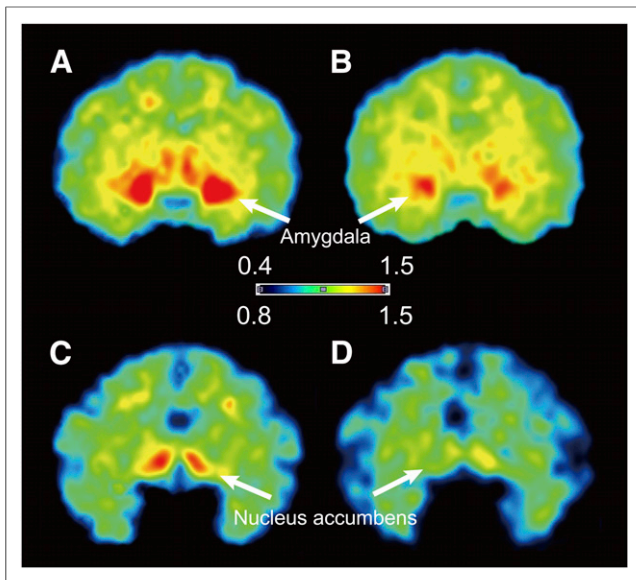


FIGURE 4. DVR images of ^{11}C -cetrozole (A and C) and ^{11}C -vorozole (B and D) in amygdala (A and B) and nucleus accumbens (C and D) of rhesus monkey (coronal slices). DVRs in amygdala and nucleus accumbens regions are 0.4–1.5 and 0.8–1.5, respectively. DVR of ^{11}C -cetrozole was higher in these regions than that of ^{11}C -vorozole.

signal-to-noise ratios (ratio of baseline to blocking) in the amygdala, hypothalamus, and nucleus accumbens: ^{11}C -cetrozole, 10.5, 5.7, and 6.3, respectively; ^{11}C -vorozole, 3.4, 1.7, and 2.6, respectively (Fig. 6).

DISCUSSION

To evaluate the *in vivo* function of aromatase playing important roles in the brain, molecular PET imaging is one of the most straightforward approaches. ^{11}C -labeled vorozole, the first aromatase inhibitor-type PET probe developed at the Uppsala University PET Centre, allowed imaging of the dynamic status of aromatase in the living body including the brain (15). PET studies using this probe clarified the distribution of aromatase in living rhesus monkeys (16,24,27), baboons (17), and also humans (18), strongly suggesting a role for aromatase in brain functions. For example, an increase in aromatase expression was detected in the hypothalamic nuclei of rats and rhesus monkeys by the repeated administration

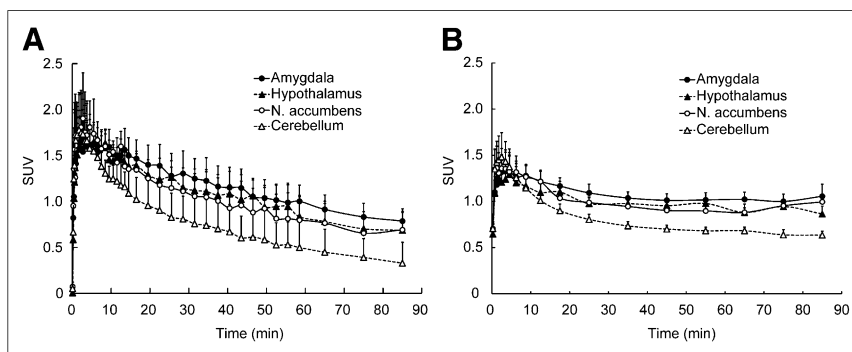


FIGURE 5. Time-activity curves of ^{11}C -cetrozole (A, $n = 4$, mean \pm SEM) and ^{11}C -vorozole (B, $n = 5$, mean \pm SEM) in rhesus monkey brain. SUV of high-binding regions (amygdala, hypothalamus, and nucleus accumbens) and reference region for Logan reference tissue model analysis (cerebellum) are shown. N. = nucleus.

of anabolic androgenic steroids for 3 wk daily, inducing psychologic adverse effects (27). However, during PET studies using ^{11}C -vorozole in rhesus monkeys, we showed increased brain SUV in the late time phase of PET scans, suggesting reuptake of the radiolabeled metabolites of ^{11}C -vorozole into the brain. Because the N- ^{11}C -methyl bond in the ^{11}C -vorozole structure was presumed to be susceptible to metabolic cleavage producing undesired ^{11}C -labeled metabolites, we designed a new PET probe with a more metabolically stable C- ^{11}C -methyl structure. On the basis of a potent aromatase inhibitor YM511 with an IC_{50} of 0.12 nM on human placental aromatase (25), we developed a new compound, ^{11}C -cetrozole, by changing the bromophenyl moiety of YM511 to ^{11}C -methylphenyl group. Cetrozole does not have an asymmetric center, making its synthesis easy, and showed potent aromatase inhibitory activity comparable with vorozole. The introduction of the ^{11}C -methyl group to the phenyl moiety was efficiently achieved using the Suzuki- or Stille-type rapid ^{11}C -methylation reaction of corresponding boryl or stannyl precursors developed by our group (Fig. 1; Supplemental Fig. 1) (26).

Metabolite analyses of plasma and brain of rats and monkeys administered ^{11}C -cetrozole or ^{11}C -vorozole revealed that both tracers were metabolized at a similar rate in plasma in both rats and monkeys. However, in the rat brain, the ^{11}C -vorozole metabolites were detected, but ^{11}C -cetrozole metabolites were not, indicating that ^{11}C -vorozole metabolites entered the brain in radiolabeled form but those of ^{11}C -cetrozole did not. This means that the PET signal from ^{11}C -vorozole originated from both the parent compound and the metabolites but that of ^{11}C -cetrozole was mostly from the parent compound. This idea was also supported by the observation of increased brain SUV for ^{11}C -vorozole in the late time phase in the rhesus monkey study; increased brain SUV was not observed in the ^{11}C -cetrozole study. These results indicated that ^{11}C -cetrozole may be a more preferable tracer than ^{11}C -vorozole for the quantitative measurement of aromatase in the brain. Even in a human PET study (18), the time-activity curve of ^{11}C -vorozole in the brain was almost the same as that of the monkey: specifically, that increased radioactivity was also observed in the late phase.

The Scatchard plot for the binding assay using the rat amygdala homogenate showed linearity of the slope, indicating that ^{11}C -cetrozole bound to a single binding site of aromatase, similar to ^{11}C -vorozole (16). The K_d value was 0.11 nM, indicating that ^{11}C -cetrozole had a higher affinity to aromatase than ^{11}C -vorozole, which has a K_d of 0.60 nM (16). The IC_{50} values obtained with the aromatase inhibition assay using marmoset placenta were 1.27 and 0.66 nM for cetrozole and vorozole, respectively (Supplemental Fig. 7). Our PET data showed binding potentials that were higher for ^{11}C -cetrozole than ^{11}C -vorozole and may represent the K_d of each compound rather than inhibitory activity. The binding of ^{11}C -cetrozole was inhibited by the administration of 1 μM unlabeled vorozole, suggesting that cetrozole binds to an androgen-specific cleft of aromatase, similar to vorozole (30).

To analyze PET data, the method of using a reference region may be less quantitative than the method of using an arterial blood sample as an input function. To explore the possibility of using reference region-based analysis for ^{11}C -cetrozole, we compared the result from the Logan reference tissue

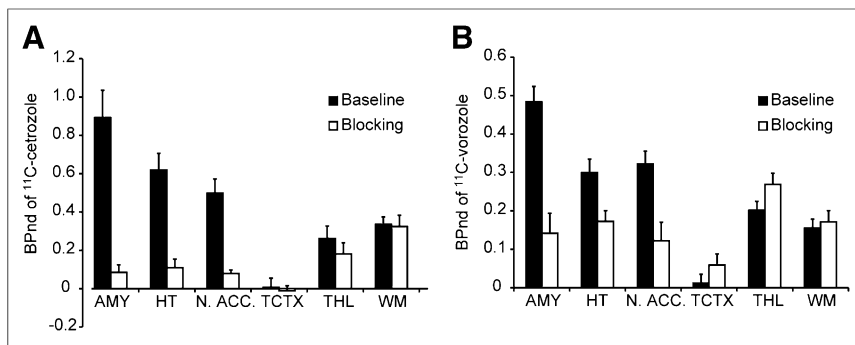


FIGURE 6. BPnd of ^{11}C -cetrozole (A, $n = 4$, mean \pm SEM) and ^{11}C -vorozole (B, $n = 5$, mean \pm SEM) with (blocking) or without (baseline) unlabeled vorozole in amygdala (AMY), hypothalamus (HT), nucleus accumbens (N. ACC.), temporal cortex (TCTX), thalamus (THL), and white matter (WM) in rhesus monkey. ^{11}C -cetrozole showed better signal-to-noise ratio than ^{11}C -vorozole in amygdala, hypothalamus, and nucleus accumbens.

model based on the average k_2' (BPnd) and that from arterial blood sampling as the input function (Vt). The cerebellum was selected as a reference region because it contains negligible amounts of aromatase messenger RNA and enzymatic activity (31). The radioactivity in all examined brain regions was reduced to the level of the cerebellum with pretreatment with an excess amount of unlabeled vorozole. Additionally, to confirm that ^{11}C -cetrozole does not specifically bind in the cerebellum, both 1-tissue- and 2-tissue-compartment models were applied to the kinetics of radioactivity in the cerebellum. The kinetics fit better with the 1-tissue-compartment model with smaller values of Akaike information criteria, suggesting the suitability of the cerebellum as the reference region. To compare the calculated with the input function of arterial blood and the BPnd determined with the Logan noninvasive model using the cerebellum as the reference region, Vts of all examined brain regions were normalized to the Vt of the cerebellum. The normalized values of Vt and BPnd were well correlated ($r > 0.99$), and the difference between these 2 values was less than 5%. Thus, the Logan noninvasive model using the cerebellum could be used for data analysis of brain PET imaging with ^{11}C -cetrozole.

As a result, high specific binding of ^{11}C -cetrozole was observed in the amygdala, hypothalamus, and nucleus accumbens. The signal-to-noise ratios of BPnd in these 3 regions were 10.4, 5.6, and 6.2, respectively, which were better than those for ^{11}C -vorozole: 3.4, 1.7, and 2.6, respectively. Early studies measuring the messenger RNA level showed that aromatase is expressed at high levels in the amygdala and hypothalamus of rhesus monkeys (31). A previous PET study with ^{11}C -vorozole showed high specific binding in the amygdala and relatively weak binding in the hypothalamus (16), results that were reproduced in this study. The present study with ^{11}C -cetrozole clearly demonstrated that the amygdala and hypothalamus contained high amounts of aromatase in the rhesus monkey brain. In addition, the nucleus accumbens was clearly delineated only with ^{11}C -cetrozole. DVR images of ^{11}C -vorozole had too-high nonspecific binding to delineate the nucleus accumbens clearly. The localization of aromatase in the nucleus accumbens was also supported by Western blotting (Takahashi et al., unpublished data, 2012). The nucleus accumbens is thought to be involved with reward, motivation, addiction, and aggression (32,33) through the dopaminergic system, which is partly modulated by estrogen (34). Therefore, aromatase in the amygdala, hypothalamus, and also the nucleus accumbens may be involved in emotional behavior. Further research is needed to clarify this idea.

CONCLUSION

We developed ^{11}C -cetrozole, which showed a higher signal-to-noise ratio suitable for the quantitative analysis of aromatase expression in the amygdala, hypothalamus, and nucleus accumbens in the brain of non-human primates. ^{11}C -cetrozole will be a powerful tool for exploring the functional roles of aromatase in human neurologic and emotional disorders.

DISCLOSURE

The costs of publication of this article were defrayed in part by the payment of page charges. Therefore, and solely to indicate this fact, this article is hereby marked "advertisement" in accordance with 18 USC

section 1734. This work was supported in part by a consignment expense for the Molecular Imaging Research Programs entitled "Research Base for Exploring New Drugs" from the Japanese Ministry of Education, Culture, Sports, Science and Technology and JSPS KAKENHI grants 22791155 and 25830024. No other potential conflict of interest relevant to this article was reported.

ACKNOWLEDGMENTS

We thank Dr. Yasuhisa Tamura, Masahiro Kurahashi, Akihiro Kawasaki, Chiho Takeda, Yumiko Katayama, Tomoko Mori, and Emi Hayashinaka (RIKEN) for their assistance with the PET study and Masayo Ishikawa (Tokyo Institute of Technology) and Ayako Hosoya (Tokyo Medical and Dental University) for HRMS analysis.

REFERENCES

- Simpson ER, Clyne C, Rubin G, et al. Aromatase: a brief overview. *Annu Rev Physiol.* 2002;64:93–127.
- Hill RA, Chua HK, Jones ME, Simpson ER, Boon WC. Estrogen deficiency results in apoptosis in the frontal cortex of adult female aromatase knockout mice. *Mol Cell Neurosci.* 2009;41:1–7.
- Hill RA, Pompolo S, Jones ME, Simpson ER, Boon WC. Estrogen deficiency leads to apoptosis in dopaminergic neurons in the medial preoptic area and arcuate nucleus of male mice. *Mol Cell Neurosci.* 2004;27:466–476.
- Azcoitia I, Sierra A, Veiga S, Honda S, Harada N, Garcia-Segura LM. Brain aromatase is neuroprotective. *J Neurobiol.* 2001;47:318–329.
- Morale MC, L'Episcopo F, Tirolo C, et al. Loss of aromatase cytochrome P450 function as a risk factor for Parkinson's disease? *Brain Res Rev.* 2008;57:431–443.
- Dalla C, Antoniou K, Papadopoulou-Daifoti Z, Balthazart J, Bakker J. Oestrogen-deficient female aromatase knockout (ArKO) mice exhibit depressive-like symptomatology. *Eur J Neurosci.* 2004;20:217–228.
- Honda S, Harada N, Ito S, Takagi Y, Maeda S. Disruption of sexual behavior in male aromatase-deficient mice lacking exons 1 and 2 of the cyp19 gene. *Biochem Biophys Res Commun.* 1998;252:445–449.
- Bakker J, Honda S, Harada N, Balthazart J. Restoration of male sexual behavior by adult exogenous estrogens in male aromatase knockout mice. *Horm Behav.* 2004;46:1–10.
- Honda S, Wakatsuki T, Harada N. Behavioral analysis of genetically modified mice indicates essential roles of neurosteroidal estrogen. *Front Endocrinol.* 2011; 2:1–8.
- Sato T, Matsumoto T, Kawano H, et al. Brain masculinization requires androgen receptor function. *Proc Natl Acad Sci USA.* 2004;101:1673–1678.
- Martin S, Jones M, Simpson E, van den Buuse M. Impaired spatial reference memory in aromatase-deficient (ArKO) mice. *Neuroreport.* 2003;14:1979–1982.
- Ishunina TA, van Beurden D, van der Meulen G, et al. Diminished aromatase immunoreactivity in the hypothalamus, but not in the basal forebrain nuclei in Alzheimer's disease. *Neurobiol Aging.* 2005;26:173–194.

13. Sarachana T, Xu M, Wu RC, Hu VW. Sex hormones in autism: androgens and estrogens differentially and reciprocally regulate RORA, a novel candidate gene for autism. *PLoS ONE*. 2011;6:e17116.
14. Garcia-Segura LM. Aromatase in the brain: not just for reproduction anymore. *J Neuroendocrinol*. 2008;20:705–712.
15. Lidström P, Bonasera TA, Kirilovas D, et al. Synthesis, in vivo rhesus monkey biodistribution and in vitro evaluation of a ¹¹C-labelled potent aromatase inhibitor: [*N*-methyl-¹¹C]vorozole. *Nucl Med Biol*. 1998;25:497–501.
16. Takahashi K, Bergstrom M, Frandberg P, Vesstrom EL, Watanabe Y, Langstrom B. Imaging of aromatase distribution in rat and rhesus monkey brains with [¹¹C]vorozole. *Nucl Med Biol*. 2006;33:599–605.
17. Kim SW, Biegion A, Katsamanis ZE, et al. Reinvestigation of the synthesis and evaluation of [*N*-methyl-¹¹C]vorozole, a radiotracer targeting cytochrome P450 aromatase. *Nucl Med Biol*. 2009;36:323–334.
18. Biegion A, Kim SW, Alexoff DL, et al. Unique distribution of aromatase in the human brain: in vivo studies with PET and [*N*-methyl-¹¹C]vorozole. *Synapse*. 2010;64:801–807.
19. Takahashi K, Hallberg M, Magnusson K, et al. Increase in [¹¹C]vorozole binding to aromatase in the hypothalamus in rats treated with anabolic androgenic steroids. *Neuroreport*. 2007;18:171–174.
20. Takahashi K, Tamura Y, Watanabe Y, Langstrom B, Bergstrom M. Alteration in [¹¹C]vorozole binding to aromatase in neuronal cells of rat brain induced by anabolic androgenic steroids and flutamide. *Neuroreport*. 2008;19:431–435.
21. Wang M, Lacy G, Gao M, Miller KD, Sledge GW, Zheng QH. Synthesis of carbon-11 labeled sulfonanilide analogues as new potential PET agents for imaging of aromatase in breast cancer. *Bioorg Med Chem Lett*. 2007;17:332–336.
22. Wang M, Mickens J, Gao M, et al. Design and synthesis of carbon-11-labeled dual aromatase-steroid sulfatase inhibitors as new potential PET agents for imaging of aromatase and steroid sulfatase expression in breast cancer. *Steroids*. 2009;74:896–905.
23. Kil KE, Biegion A, Ding YS, et al. Synthesis and PET studies of [¹¹C-cyano]letrozole (Femara), an aromatase inhibitor drug. *Nucl Med Biol*. 2009;36:215–223.
24. Takahashi K, Yamagishi G, Hiramatsu T, et al. Practical synthesis of precursor of [*N*-methyl-¹¹C]vorozole, an efficient PET tracer targeting aromatase in the brain. *Bioorg Med Chem*. 2011;19:1464–1470.
25. Okada M, Yoden T, Kawaminami E, et al. Studies on aromatase inhibitors. I. Synthesis and biological evaluation of 4-amino-4*H*-1,2,4-triazole derivatives. *Chem Pharm Bull (Tokyo)*. 1996;44:1871–1879.
26. Doi H, Ban I, Nonoyama A, et al. Palladium(0)-mediated rapid methylation and fluoromethylation on carbon frameworks by reacting methyl and fluoromethyl iodide with aryl and alkenyl boronic acid esters: useful for the synthesis of [¹¹C]CH₃-C- and [¹⁸F]FCH₂-C-containing PET tracers (PET=positron emission tomography). *Chem Eur J*. 2009;15:4165–4171.
27. Takahashi K, Onoe K, Doi H, et al. Increase in hypothalamic aromatase in macaque monkeys treated with anabolic-androgenic steroids: PET study with [¹¹C]vorozole. *Neuroreport*. 2011;22:326–330.
28. Logan J, Fowler JS, Volkow ND, et al. Graphical analysis of reversible radioligand binding from time-activity measurements applied to [*N*-¹¹C-methyl]-(-)-cocaine PET studies in human subjects. *J Cereb Blood Flow Metab*. 1990;10:740–747.
29. Logan J, Fowler JS, Volkow ND, Wang GJ, Ding YS, Alexoff DL. Distribution volume ratios without blood sampling from graphical analysis of PET data. *J Cereb Blood Flow Metab*. 1996;16:834–840.
30. Ghosh D, Griswold J, Erman M, Pangborn W. Structural basis for androgen specificity and oestrogen synthesis in human aromatase. *Nature*. 2009;457:219–223.
31. Abdelgadir SE, Roselli CE, Choate JV, Resko JA. Distribution of aromatase cytochrome P450 messenger ribonucleic acid in adult rhesus monkey brains. *Biol Reprod*. 1997;57:772–777.
32. Di Chiara G, Bassareo V. Reward system and addiction: what dopamine does and doesn't do. *Curr Opin Pharmacol*. 2007;7:69–76.
33. Beiderbeck DI, Reber SO, Havasi A, Bredewold R, Veenema AH, Neumann ID. High and abnormal forms of aggression in rats with extremes in trait anxiety: involvement of the dopamine system in the nucleus accumbens. *Psychoneuroendocrinology*. 2012;37:1969–1980.
34. Le Saux M, Morissette M, Di Paolo T. ERbeta mediates the estradiol increase of D2 receptors in rat striatum and nucleus accumbens. *Neuropharmacology*. 2006;50:451–457.